The Algorithms of the Cross-Coupled Precompensation Method for Generating the Involute-Type Scrolls

Jih-Hua Chin
Professor.

Hu-Wai Lin
Graduate Student.

Department of Mechanical Engineering,
National Chiao Tung University,
Hsinchu, Taiwan

Cross-coupled precompensation method (CCPM) has been proven efficient in tracking nonlinear spatial curves. It requires a path generating algorithm derived from the mathematical equation of the target curve. This paper discussed the time base transform of target curve from a parametric form. The time based path generating algorithm for the extended involute scroll was then proposed. A comparison among three kinds of tool path generating algorithms were performed. The proposed path algorithms, along with other two algorithms, were implemented and tracked by four different control schemes, US (uncoupled-unprecompensated system), CCS (cross-coupled system), PPM (path precompensation method), and cross-coupled precompensation method (CCPM). The proposed path algorithm for extended involute scroll provided the best accuracy. The proposed algorithm tracked by CCPM achieved the most precise profile especially at high feedrates.

1 Introduction

In computerized numerical control (CNC) technology the term "position error" means the error between actual and desired position while the "contour error" is used to express the error component orthogonal to the desired trajectory. In fact the contour error is often of more concern during the manufacturing process, since it spells the error of profile. There are products of which the profiles are extremely important; one industrial example is the scroll of compressors. The scroll compressor has been widely used due to its high efficiency and reliability, low vibration and noise as well as its contribution to the environmental protection (Ishii et al., 1990). Most of the scrolls are mathematically represented by the standard involute curve which builds a serious challenge to the CNC machine tools.

As far as the accurate contouring is concerned, the cross-coupled control system has been proven effective for certain trajectories in biaxial machine tools. Koren (1980) proposed a cross-coupled biaxial system with the addition of two DDA integrators and a digital comparator to a conventional biaxial control system. They have improved the limitation of nonsymmetrical cross-coupled system and steady-state contour error. Kulkarni and Srinivasan (1989) proposed a cross-coupled controller which involves an optimal control to improve high-speed contouring accuracy. Koren and Lo (1991) proposed a variable gain cross-coupled controller to deal with nonlinear contour such as circle and parabola. Chung and Liu (1991, 1992) proposed an adaptive feedrate control and model-reference adaptive control strategy. Huang and Chen (1995) proposed an application of cross-coupled control in a retrofitted milling machine.

Parallel to the cross-coupled concept another path method was proposed (Chin and Tsai, 1993) to increase the contour accuracy in which the path parameters are preadapted before the tracking. The algorithm which was adapted from Huan (1982) was named as the PPM (Path Precompensation Method). Chin and Lin (1997) applied the PPM to the flexible arm to track a path for better precision. Chin and Tsai (1997) proposed algorithms for PPM for tracking spatial curves in parameter form. Since a velocity modification is executed before trajectory tracking, and the most parts of motion mechanism are included within the feedback loop, the PPM has been proven accurate in tracking curvilinear trajectories.

Recently, Chin and Lin (1997) made a combination of cross-coupled system and PPM to reach the best contouring accuracy among several methods. Chin and Liu (1997) advanced the cross-coupled precompensation method for tracking higher order curves by cubic spline fitting. The combination of the cross-coupled concept and the precompensation method has displayed a powerful ability in reducing the contour error for paths with curvature, especially at high feedrates of up to 200 mm/sec. The reason for its outstanding performance is that specific equations were derived from exact mathematical equation of target curve so that accuracy is sustained from the beginning, and the accuracy is then held tightly by both features of cross-coupling and precompensation.

This study investigated the path planning and control strategy for the scroll profile which is mathematically described by the extended involute curve. Time-based equations were derived from the extended involute curve for tracking purposes. The experiment was implemented by three kinds of path planning: (*i*) our proposed algorithm which was determined by time and feedrate, (*ii*) the method proposed by Chin and Liu (1997) which uses cubic spline fitting, (*iii*) the method proposed by Shpitalni et al. (1994). The path planning algorithms were combined with four kinds of control schemes: US (uncoupled-unprecompensated system), CCS (cross-coupled system), PPM (Path precompensation method), CCPM (cross-coupled precompensation method) to compare the tracking accuracy of the trajectory. Note that in this study, the contour error was the shortest distance between the actual position and the contour itself calculated by a minimization process, instead of an approximate value used by Kulkarni and Srinivasan (1990) which was the distance from the actual position to the tangent of the desired contour, as shown in Fig. 1.

2 The Tool Path Algorithms

2.1 Time Base Consideration. In order to deal with spatial curves, the parameter form of a target curve is adopted by

Contributed by the Dynamic Systems and Control Division for publication in the JOURNAL OF DYNAMIC SYSTEMS, MEASUREMENT, AND CONTROL. Manuscript received by the Dynamic Systems and Control Division December 18, 1997. Associate Technical Editor: T. Kurfess.

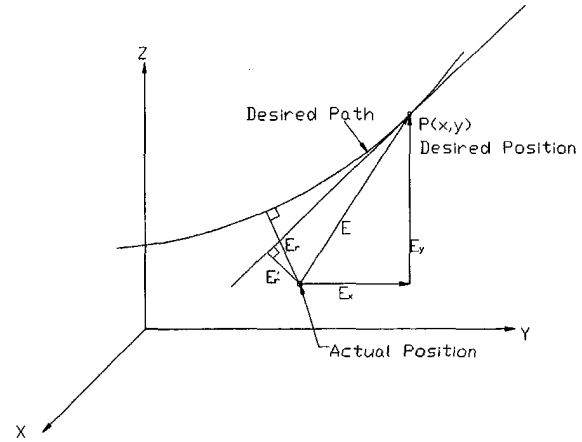

Fig. 1 The approximate contour error E_r' and actual contour error E_r for a curve contour

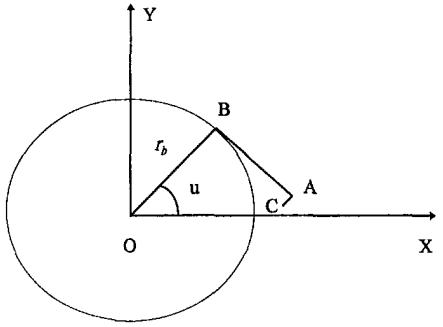

Fig. 2 The generation of an extended involute curve

Chin and Liu (1997), and Chin and Tsai (1997). A spatial curve can be made represented by a set of parametric equations $x(u)$, $y(u)$, $z(u)$ with a curve parameter u as follows:

$$\mathbf{P}(u) = x(u)\mathbf{i} + y(u)\mathbf{j} + z(u)\mathbf{k} \tag{2.1}$$

where $\mathbf{P}(u)$ is the arbitrary position vector of a spatial curve.

In a CNC machine tool however, the trajectory has to be written as a function of time for the sake of control, since the displacement of cutter should be equivalent in each sampling time. So Eq. (2.1) shall be considered in time base. The time required by a cutter to travel along a trajectory from u_0 to u is

$$t = \int_{u_0}^{u} \frac{ds(u)}{V(u)} = \int_{u_0}^{u} \frac{\sqrt{\left(\frac{dx}{du}\right)^2 + \left(\frac{dy}{du}\right)^2 + \left(\frac{dz}{du}\right)^2}}{V(u)}\, du \tag{2.2}$$

where $ds(u)$ denotes the differential length of the trajectory and $V(u)$ represents the magnitude of feedrate of the cutter with $V(u) = \sqrt{(dx(u)/du)^2 + (dy(u)/du)^2 + (dz(u)/du)^2}\, du/dt$.

Here we have

$$\frac{du}{dt} = \frac{V(u)}{\sqrt{\left(\frac{dx(u)}{du}\right)^2 + \left(\frac{dy(u)}{du}\right)^2 + \left(\frac{dz(u)}{du}\right)^2}} \tag{2.3}$$

Equation (2.2) is difficult to solve, since its right term is usually an integral of a nonlinear equation, so we use Eq. (2.3) and a simpler first order difference equation (Isermann, 1987):

$$du(t)/dt \approx [u(k\cdot T) - u((k-1)\cdot T)]/T \tag{2.4}$$

where T is the sampling time.

Considering both Eqs. (2.3) and (2.4), a discrete form of u is obtained as follows:

Note that Eq. (2.5) is an approximation which is equivalent to expand $u(t)$ into Taylor's series:

$$u(t) = u(t_0) + \frac{du}{dt}(t - t_0) + \frac{1}{2!}\frac{d^2u}{dt^2}(t - t_0)^2 + \ldots.$$

and then take only the first two terms of the expansion (Isermann, 1987). If Eq. (2.5) is used to describe the whole curve and $t_0 = 0$ then k increases monotonously from 1 to n. After iterative computations, we can obtain the tool path in terms of time parameter t instead of curve parameter u

$$\mathbf{P}(t_n) = x(t_n)\mathbf{i} + y(t_n)\mathbf{j} + z(t_n)\mathbf{k} \tag{2.6}$$

where t_n is the elapsed time of n sampling time (i.e., $t_n = n\cdot T$).

2.2 Path Algorithm for the Extended Involute. An extended involute is generated by a point which is unwrapped from a base circle with an extended segment as shown in Fig. 2. The line $\overline{AC}$ in Fig. 2 is perpendicular to line $\overline{AB}$. When line $\overline{AB}$ is unwrapped from the base circle, the locus of point A produces a standard involute while the locus of point C produces an extended involute. The extended involute scroll has better hermetic characteristics than the standard involute scroll when taking into account the influence of temperature and pressure loads, and the optimized extended involute scroll can reduce the leakage (Tseng and Shih, 1995). From the geometrical point of view, the extended involute scroll is more applicable since the standard involute was only a special case of the extended involute.

The representation of the extended involute curve is as follows:

$$\mathbf{P} = (-D\cos u + r_b\cos u + r_b u\sin u)\mathbf{i} + (-D\sin u + r_b\sin u - r_b u\cos u)\mathbf{j} \tag{2.7}$$

where r_b is the radius of base circle and D is the length of the extended segment of $\overline{AC}$ and u is the involute angle formed by line $\overline{OB}$ and the x-axis. Note that when $D = 0$ it becomes a standard involute curve.

$$u(k\cdot T) = u((k-1)\cdot T) + \frac{V(u((k-1)\cdot T))}{\sqrt{\left(\frac{dx(u((k-1)\cdot T))}{du}\right)^2 + \left(\frac{dy(u((k-1)\cdot T))}{du}\right)^2 + \left(\frac{dz(u((k-1)\cdot T))}{du}\right)^2}} T, \quad 1 \le k \le n \tag{2.5}$$

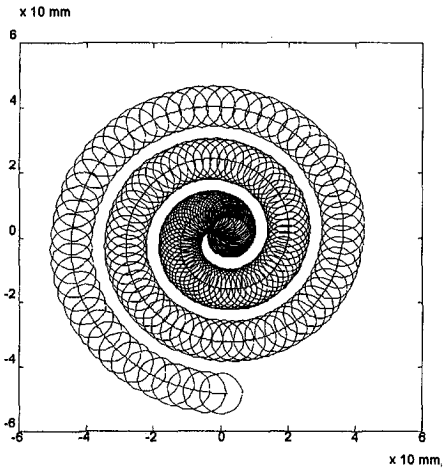

Fig. 3 The locus of the tool path and the profile of the scroll. D = 0.1 mm r_b = 2.578 mm r_t = 6.3 mm

As shown in Fig. 3, the scroll is the remainder after the tool cutting. The profile of the scroll is generated by the locus of the cutting tool which is represented by Eq. (2.7) plus a tool shape vector. By using the fact that the unit normal vector of tool shape is always orthogonal to the relative velocity of the tool, the representation of the outer and inner profile of scroll can be obtained as follows (Tseng and Lia, 1994):

$$\mathbf{P}_o = [(r_b - D)\cos u + r_b u \sin u + r_t \cos \Psi]\mathbf{i} + [(r_b - D)\sin u - r_b u \cos u + r_t \sin \Psi]\mathbf{j}$$

$$\mathbf{P}_i = [(r_b - D)\cos u + r_b u \sin u + r_t \cos(\Psi + \pi)]\mathbf{i} + [(r_b - D)\sin u - r_b u \cos u + r_t \sin(\Psi + \pi)]\mathbf{j} \quad (2.8)$$

where $\Psi = u + \tan^{-1}(r_b u/D)$ and r_t is the radius of tool.

From a control point of view, we can concentrate on the locus of cutting tool to produce the profile of scroll. Let $\mathbf{P}_i$ denote the actual position vector, the position error can be represented by $\mathbf{E} = \mathbf{P}_i - \mathbf{P}$, the magnitude of which is

$$E = [r_b^2 + r_b^2 u^2 + D^2 + x_i^2 + y_i^2 - 2r_b D - 2r_b(x_i \cos u + y_i \sin u) + 2r_b u(y_i \cos u - x_i \sin u) + 2D(x_i \cos u + y_i \sin u)]^{1/2} \quad (2.9)$$

Let $E' = 0$ and use the "Modified Flase Method" (Nakamura, 1993), a u^* can be found which makes $\mathbf{P}(u^*)$ the closest point to the actual position $\mathbf{P}_i$. The "contour error" E_r which is the smallest distance between the actual position $\mathbf{P}_i(x_i, y_i)$ and the point on the spatial curve $P(x(u^*), y(u^*))$, is the component of the position error that's orthogonal to the desired path.

$$E_r = |\mathbf{P}(\mathbf{u}^*) - \mathbf{P}_i| = \sqrt{(x(u^*) - x_i)^2 + (y(u^*) - y_i)^2}$$
$$= \sqrt{[r_b(\cos u^* + u^* \sin u^*) - D\cos u^* - x_i]^2 + [r_b(\sin u^* - u^* \cos u^*) - D \sin u^* - y_i]^2} \quad (2.10)$$

The geometric formula derived above is less applicable for the tool path in terms of curve parameter u because it will cause inconstant feedrate. It is desirable that the feedrate be maintained constant. Consequently, it is necessary to transform curve parameter u to time parameter t. The time required for the cutter to track the trajectory from u_0 to u is

$$t = \int_{u_0}^{u} \frac{\sqrt{\left(\frac{dx}{du}\right)^2 + \left(\frac{dy}{du}\right)^2}}{V(u)}\, du = r_b \int_{u_0}^{u} \frac{\sqrt{u^2 + \left(\frac{D}{r_b}\right)^2}}{V(u)}\, du \quad (2.11)$$

The feedrate $V(u)$ is usually a constant, that is $V(u) = V$.

If the locus of tool path starts from the origin, the relationship between curve parameter u and time parameter t derived for Eq. (2.11) is

$$t = \frac{u}{2V}\sqrt{u^2 + \left(\frac{D}{r_b}\right)^2} + \frac{1}{2}\left(\frac{D}{r_b}\right)^2 \ln\left|u + \sqrt{u^2 + \left(\frac{D}{r_b}\right)^2}\right| - \frac{1}{2}\left(\frac{D}{r_b}\right)^2 \ln\left|\frac{D}{r_b}\right| \quad (2.12)$$

Consequently we can obtain the representation of the time-based extended involute curve:

$$P(t) = x(t)\mathbf{i} + y(t)\mathbf{j}$$

where t is given by Eq. (2.12).

A function of curve parameter u in terms of time parameter t can be obtained by first calculating du/dt from Eq. (2.7) and (2.3) which gives $du/dt = V(u)/\sqrt{r_b^2 u^2 + D^2}$, and then substituting this du/dt into Eq. (2.5) which yields:

$$u(k \cdot T) = u((k-1)\cdot T) + \left[\frac{V(u((k-1)T))}{\sqrt{r_b^2 u^2((k-1)T) + D^2}}\right] \cdot T, \quad 1 \le k \le n \quad (2.13)$$

Thus, the arbitrary position vector of extended involute curve can be represented as

$$\mathbf{P}(u(t_n)) = x(u(t_n))\mathbf{i} + y(u(t_n))\mathbf{j} = [(r_b - D)\cos u(t_n) + r_b u(t_n)\sin u(t_n)]\mathbf{i} + [(r_b - D)\sin u(t_n) - r_b u(t_n)\cos u(t_n)]\mathbf{j} \quad (2.14)$$

Equation (2.14) is the tool-path generator for the extended involute scroll which allows rapid and accurate tool locus generation.

2.3 Extended Involute Fitted by the Spatial Cubic Spline. A spatial curve can be fit by piecewise segments together with some boundary conditions. Chin and Tsai (1997) discussed spatial cubic splines for PPM. The normalized cubic spline segment they used between two points are represented by

$$P_k(u) = \sum_{i=1}^{4} B_{ik} u^{i-1} \quad 0 \le u \le 1,\ 1 \le k \le n-1 \quad (2.15)$$

where B_{ik} are the vector equivalents of the third degree polynomial, and $P_k(u)$ are any position vector on the curve segment.

The contour error of curve fitting can be reduced by choosing the start and end point. Let the starting point of the first segment

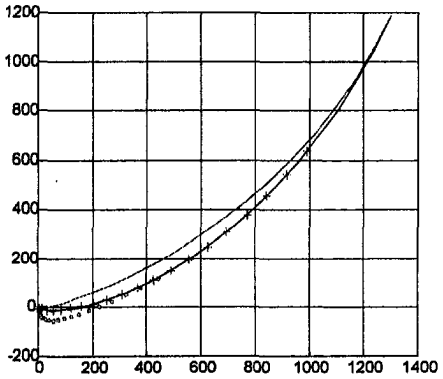

Fig. 4 Fitting deviations of different cubic splines. spline 1: . . . spline 2: + spline 3: - · - · extended involute :–

be the origin, the end point of the first segment can be obtained from Eq. (2.7) by selecting the parameter u of extended involute curve. The obtained first cubic spline segment varied with the position and slope of selected end point. By adjusting the end point, we can get the optimized first cubic spline segment with a minimum contour error. Then, take the end point of the first cubic spline segment as the start point of the second cubic spline segment, the end point of the second segment can be determined in a similar way. Proceeding in this way, a tool path can be produced by cubic spline fitting. In this section the extended involute was fit by many cubic spline segments which were adjusted to have the minimum contour errors. Figure 4 shows the possible deviations produced by different spline fittings in which spline 2 was optimized by adjusting the end point while spline 1 and 3 were not optimized.

2.4 Shpitalni et al.'s Interpolation Method for the Extended Involute Curve. Shpitalni et al. (1994) proposed an interpolation method as shown in Fig. 5. Assume the current reference position vector is $\mathbf{P}_k(\mathbf{x}_k, \mathbf{y}_k)$, the next position vector $\mathbf{P}_{k+1}(\mathbf{x}_{k+1}, \mathbf{y}_{k+1})$ is specified by the position vector of the current reference position vector and its intrinsic property (i.e., slope, curvature). For the sake of comparison Shpitalni et al.'s method is written as following:

$$\mathbf{P}_{k+1} = \mathbf{P}_k + VT \cdot \mathbf{T}_k + \overline{AB} \cdot \mathbf{N}_k \tag{2.16}$$

where $\overline{AB} = (VT)^2/2\rho_k$ is an approximate value, and $\mathbf{N}$ is the principal normal vector.

Note that the magnitude of $\overline{AB}$ varies with the sampling time T, feedrate V and curvature ρ_k. The next reference position $\mathbf{P}_{n+1}$ is represented by

$$\mathbf{P}_{n+1} = \begin{bmatrix} \mathbf{x}_{n+1} \\ \mathbf{y}_{n+1} \end{bmatrix} = \begin{bmatrix} \mathbf{x}_n \\ \mathbf{y}_n \end{bmatrix} + VT \begin{bmatrix} \mathbf{T}_x \\ \mathbf{T}_y \end{bmatrix} + \overline{AB} \begin{bmatrix} \mathbf{N}_x \\ \mathbf{N}_y \end{bmatrix} \tag{2.17}$$

where

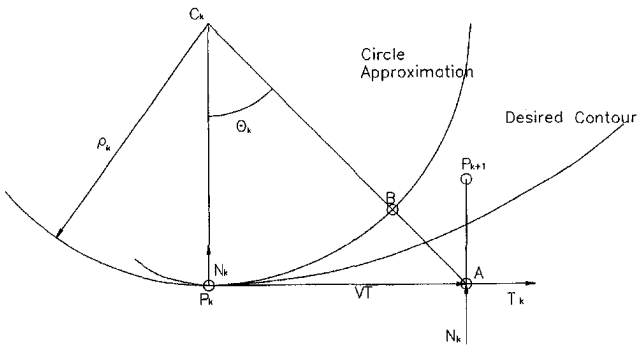

Fig. 5 Geometric relation between current and next reference positions

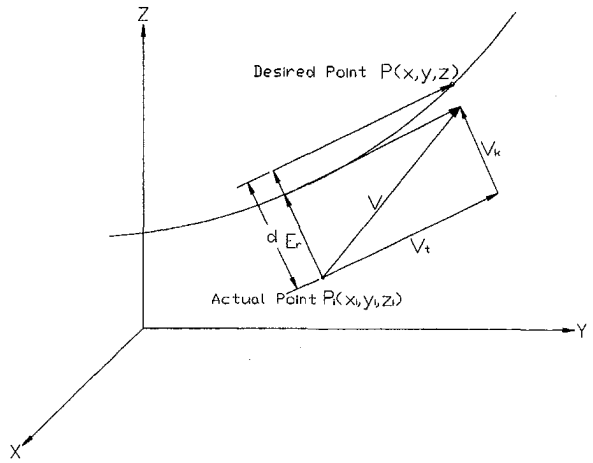

Fig. 6 Path regulation for precompensation

$$\mathbf{T} = \mathbf{T}_x + \mathbf{T}_y = \frac{(r_b u \cos u + D \sin u)}{\sqrt{r_b^2 u^2 + D^2}} \mathbf{i} + \frac{(r_b u \sin u - D \cos u)}{\sqrt{r_b^2 u^2 + D^2}} \mathbf{j}$$

Since the $\mathbf{P}_{n+1}$ is determined by feedrate and curvature, the interpolation method proposed by Shpitalni et al. (1994) may be unsuitable under the condition of high feedrate and large curvature. As shown in Fig. 5, the high feedrate and large curvature cause an increase in contour error in the resultant path. Also, for a three-dimensional curve, the determination of the magnitude of $\overline{AB}$, and the reference position $\mathbf{P}_{n+1}$ is difficult.

2.5 The Control Strategy of the Cross-Coupled Precompensation Method. The concept of path precompensation method (Chin and Tsai, 1993) is shown in Fig. 6. Let $\mathbf{V}_t$ denotes the tangent component of feedrate, and $\mathbf{V}_k$ denotes the correction velocity.

$$d = V_k \cdot T = K_v \cdot E_r$$

the correction gain is

$$K_v = \frac{d}{E_r} \tag{2.18}$$

and the idea for path precompensation is to let

$$\mathbf{V} = \mathbf{V}_t + \mathbf{V}_k = V_b \mathbf{T} + K_v \cdot \mathbf{E}_r \tag{2.19}$$

where V_b is the feedrate and $\mathbf{T}$ is the unit tangent vector.

The Cross-Coupled Precompensation System proposed by Chin and Lin (1997) has the intention of combining the advantages of the Cross-Coupled System (Koren, 1980) and the PPM (Chin and Tsai, 1993). The block diagram of a Cross-Coupled Precompensation System is shown in Fig. 7. It is seen from

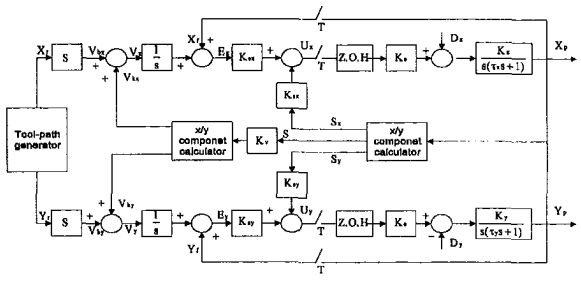

Fig. 7 Block diagram of a cross-coupled precompensation system (Chin and Lin, 1997)

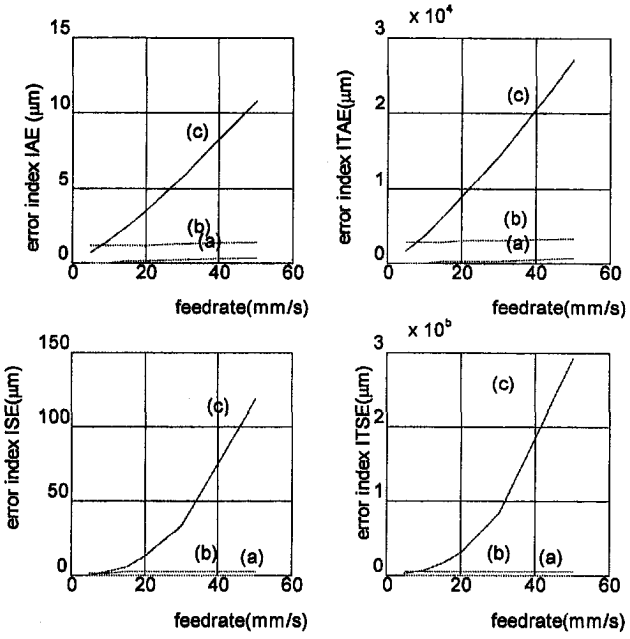

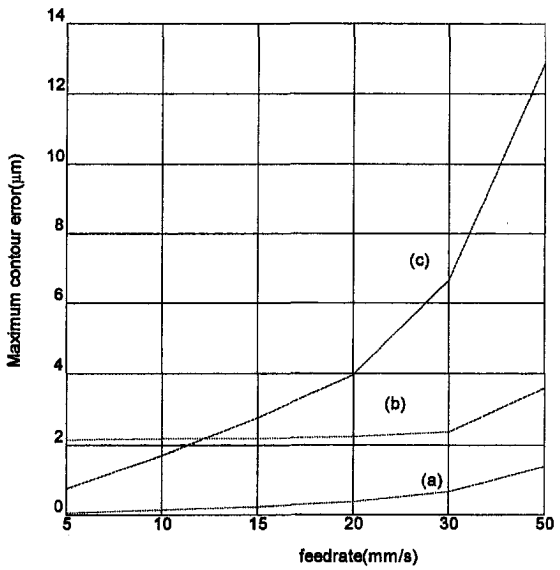

Fig. 8 The $|\epsilon_{max}|$ and error index of three kinds of tool-path. (*a*) Tool-path generated by extended involute as represented by Eq. (2.13); (*b*) tool-path generated by cubic spline fitting; (*c*) tool-path generated by Shpitalni et al.'s circular interpolation.

Fig. 7 and Eq. (2.19) that for three dimensional environment the adjusted velocities are

$$V_x(n) = V_{bx}(n-1) + K_V S_x(n)$$
$$V_y(n) = V_{by}(n-1) + K_V S_y(n)$$
$$V_z(n) = V_{bz}(n-1) + K_V S_z(n) \qquad (2.20)$$

where S_x, S_y, and S_z denote the contour error in X-, Y-, and Z-component. The position errors are

$$E_x(n) = E_x(n-1) + x_f(n) - x_p(n)$$
$$E_y(n) = E_y(n-1) + y_f(n) - y_p(n)$$
$$E_z(n) = E_z(n-1) + z_f(n) - z_p(n) \qquad (2.21)$$

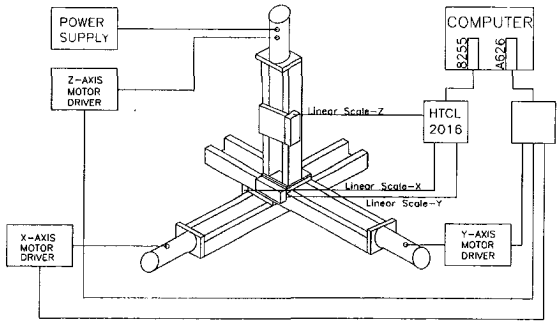

Fig. 9 View of the experimental apparatus

where x_f, y_f, and z_f are the reference positions, and x_p, y_p, and z_p are the actual position.

The control signals are

$$U_x(n+1) = K_{ex}E_x(n) + K_{sx}S_x(n)$$
$$U_y(n+1) = K_{ey}E_y(n) + K_{sy}S_y(n)$$
$$U_z(n+1) = K_{ez}E_z(n) + K_{sz}S_z(n) \qquad (2.22)$$

Note if the correction gain K_v is set to zero, the cross-coupled precompensation system reduces to a cross-coupled system. If the control gains K_{sx}, K_{sy}, and K_{sz} are set to zero, the cross-coupled precompensation system reduces to a path precompensation system, and if the correct gain K_v and the control gain K_{sx}, K_{sy}, and K_{sz} are all set to zero, the cross-coupled precompensation system reduces to an uncoupled-unprecompensated system (US).

3 Simulation

Three methods for generating the extended involute scroll were compared: (*a*) the proposed method which generates the tool-path by extended involute curve itself as described in Eq. (2.14), (*b*) the cubic spline fitting as described in Section 2.3, and (*c*) the method proposed by Shpitalni et al. (1994) which generates the tool path by circular interpolation as described in Eq. (2.17). The three kinds of tool-path planning were simulated at feedrates of 5, 10, 15, 20, 30, 50 mm/s and a sampling time of $T = 0.005$ s. We take the maximum contour error during each sampling as the contour error of its sampling term. The simulation results were quantified by "integral absolute-error (IAE) criterion," "integral-of-time-multiplied absolute-error (ITAE) criterion," "integral square-error (ISE) criterion," "integral-of-time-multiplied (ITSE) criterion." They were defined as

$$\text{IAE} = \frac{1}{N}\sum_{i=1}^{N}|S(i)|, \quad \text{ITAE} = \frac{1}{N}\sum_{i=1}^{N} t(i)|S(i)|,$$
$$\text{ISE} = \frac{1}{N}\sum_{i=1}^{N} S^2(i), \quad \text{ITSE} = \frac{1}{N}\sum_{i=1}^{N} t(i)\cdot S^2(i)$$

where $S(i)$ is the contour error of ith sampling term.

All these error indexes of IAE, ITAE, ISE, ITSE refer to the value of contour error already appeared in the stage of tool path generating.

3.1 Discussion for Simulation. The tool-path produced by the proposed method, i.e., Eq. (2.14), is determined only by the feedrate V and sampling time T. As shown in Fig. 8, the tool path generated by the time-based extended involute has the smallest $|\epsilon_{max}|$ 0.0558, 0.1285, 0.2327, 0.3556, 0.6488, 1.3883 μm at feedrate 5, 10, 15, 20, 30, 50 mm/sec respectively among three kinds of tool-path generation. The $|\epsilon_{max}|$ appear around the starting point and increase with feedrate because of the large curvature of the extended involute around the origin. For the

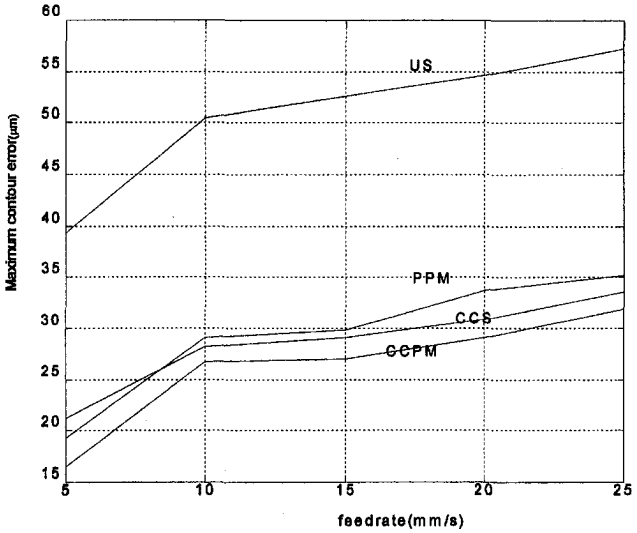

Fig. 10 The maximum contour error of US, PPM, CCS, and CCPM obtained by tracking the tool-path generated by extended involute

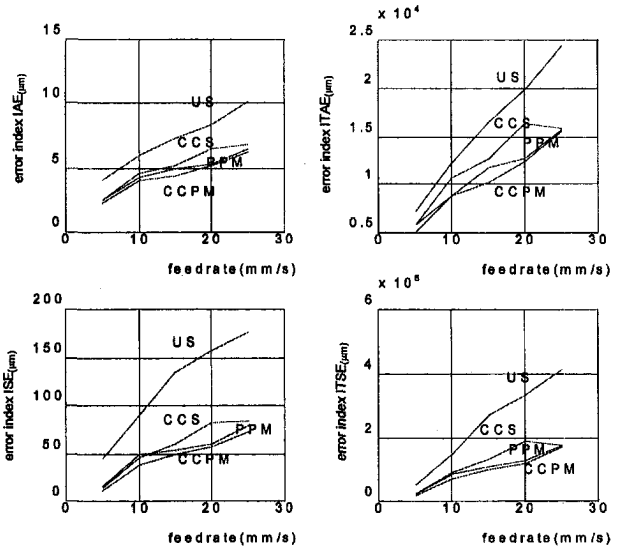

Fig. 13 The error index of US, PPM, CCS, and CCPM for tool-path generated by cubic spline

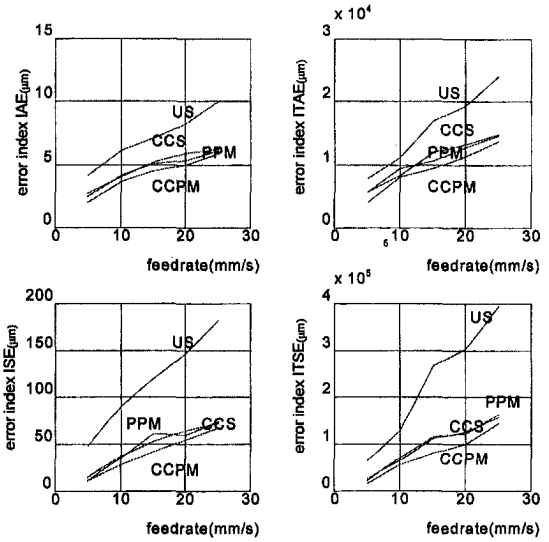

Fig. 11 Error Index of US, PPM, CCS, and CCPM obtained by tracking the tool-path generated by extended involute

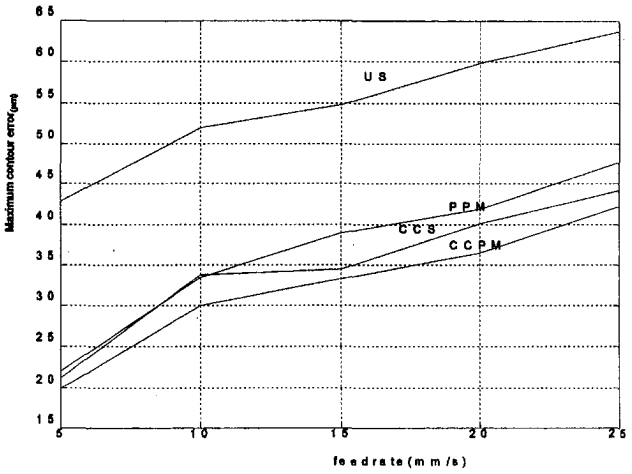

Fig. 14 The maximum contour error of US, PPM, CCS, and CCPM obtained by tracking the tool-path generated by Shpitalni et al.'s circular interpolation

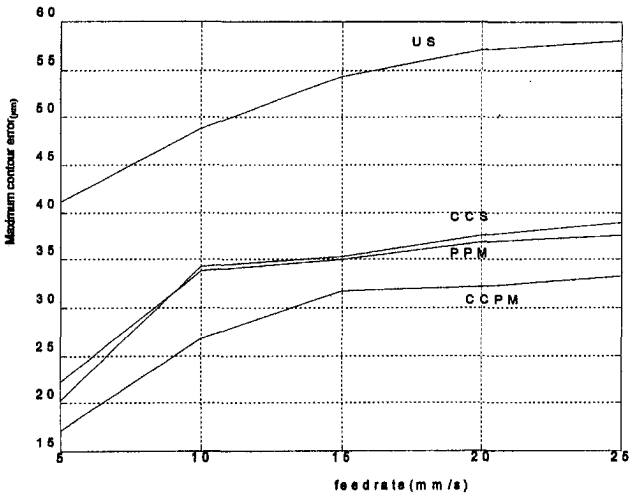

Fig. 12 The maximum contour error of US, PPM, CCS, and CCPM for tool-path generated by cubic spline

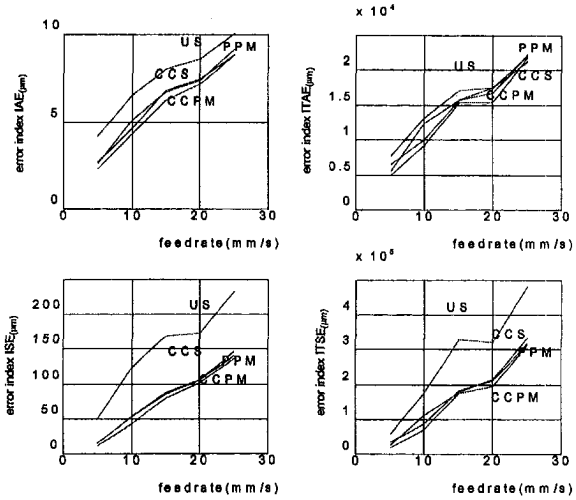

Fig. 15 The error index of US, PPM, CCS, and CCPM obtained by tracking the tool-path generated by Shpitalni et al.'s circular interpolation

Table 1 Experimental comparison by error index ratio CCPM/US at feedrate 10 mm/s

Tool path	$\lvert\epsilon_{max}\rvert_{CCPM}/\lvert\epsilon_{max}\rvert_{US}$	IAE_{CCPM}/IAE_{US}	$ITAE_{CCPM}/ITAE_{US}$	ISE_{CCPM}/ISE_{US}	$ITSE_{CCPM}/ITSE_{US}$
(a)	0.52	0.60	0.71	0.30	0.41
(b)	0.54	0.67	0.72	0.42	0.5
(c)	0.58	0.66	0.70	0.35	0.40

Table 2 Experimental comparison by error index ratio CCPM/CCS at feedrate 10 mm/s

Tool path	$\lvert\epsilon_{max}\rvert_{CCPM}/\lvert\epsilon_{max}\rvert_{CCS}$	IAE_{CCPM}/IAE_{CCS}	$ITAE_{CCPM}/ITAE_{CCS}$	ISE_{CCPM}/ISE_{CCS}	$ITSE_{CCPM}/ITSE_{CCS}$
(a)	0.9	0.89	0.83	0.79	0.75
(b)	0.78	0.89	0.83	0.83	0.81
(c)	0.89	0.85	0.74	0.81	0.62

Table 3 Experimental comparison by error index ratio CCPM/PPM at feedrate 10 mm/s

Tool path	$\lvert\epsilon_{max}\rvert_{CCPM}/\lvert\epsilon_{max}\rvert_{PPM}$	IAE_{CCPM}/IAE_{PPM}	$ITAE_{CCPM}/ITAE_{PPM}$	ISE_{CCPM}/ISE_{PPM}	$ITSE_{CCPM}/ITSE_{PPM}$
(a)	0.92	0.92	0.96	0.77	0.83
(b)	0.79	0.85	0.79	0.84	0.80
(c)	0.89	0.84	0.70	0.84	0.4

Table 4 The experimental comparison of different tool-path tracked by CCPM

Feedrate (mm/s)	$\lvert\epsilon_{max}\rvert_{(a)}/\lvert\epsilon_{max}\rvert_{(b)}$	$IAE_{(a)}/IAE_{(b)}$	$ITAE_{(a)}/ITAE_{(b)}$	$ISE_{(a)}/ISE_{(b)}$	$ITSE_{(a)}/ITSE_{(b)}$
5	0.96	0.89	0.79	0.95	0.77
10	0.97	0.9	0.9	0.73	0.73
15	0.82	0.93	0.93	0.78	0.79
20	0.9	0.97	0.90	0.96	0.82
25	0.96	0.95	0.88	0.92	0.82

tool-path generated by time-based extended involute, the $|\epsilon_{max}|$ at 50 mm/s is 1.3883 μm, which is only a fraction of 39 percent of tool-path generated by cubic spline (3.5816 μm) and 11 percent of tool-path generated by Shpitalni et al.'s circular interpolation (12.8727 μm). From comparison plotted in Fig. 8, all of the $|\epsilon_{max}|$ and error indices of IAE, ITAE, ISE, ITSE of tool-path generated by extended involute were the smallest.

The simulation results confirmed that the tool path generated by specifically derived Eq. (2.14) for extended involute has better precision, especially for higher feedrate. The tool-path generated by cubic spline fitting is determined by the geometric properties of the extended involute curve, including position vector and tangent vector. The contour error of the generated curve is dependent on the selection of end point. By adjusting the position of end points, the best cubic spline which guarantees the smallest contour error as shown in Fig. 4 can be obtained. Even so, the tool-path generated by cubic spline fitting has larger contour error than the tool-path generated by time-based extended involute as shown in Fig. 8. The tool-path generated by circular interpolation proposed by Shpitalni et al. (1994) was influenced upon by large curvature and high feedrate. The contour error increased rapidly with small increment of curvature and feedrate. It is seen that Shpitalni et al.'s method has two disadvantages in dealing with nonlinear curve like this extended involute scroll, one is the large contour error resulting from large curvature and high feedrate, the other is the difficulty in dealing with spatial curve, since the term $\overline{AB}$ is difficult to determine.

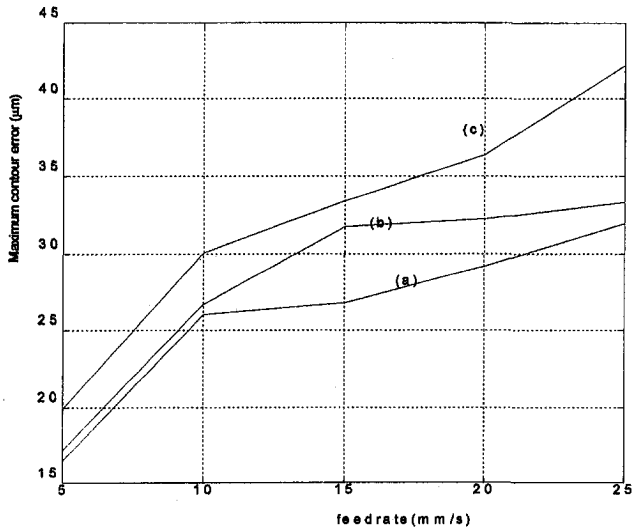

Fig. 16 The maximum contour error of three kinds of tool-path obtained by CCPM tracking. Path was generated by (*a*) extended involute, (*b*) cubic spline fitting, (c) circular interpolation (Shpitalni et al., 1994).

4 Experimental Study

In this part, four kinds of control schemes, namely US (uncoupled-unprecompensated system), CCS (cross-coupled system), PPM (path precompensation method), cross-coupled path precompensation method (CCPM) were implemented to track three kinds of tool-paths generated as described previously.

4.1 Experiment Instrument. The schema of the experimental equipment is shown in Fig. 9. The instruments of experiment are as follows:

1. Personal computer with Intel CPU 80486.
2. 600 mm × 600 mm × 300 mm X-Y-Z table with (*i*) three linear scales of 1 μm resolution (*ii*) three linear guideways of 10 mm/rev lead

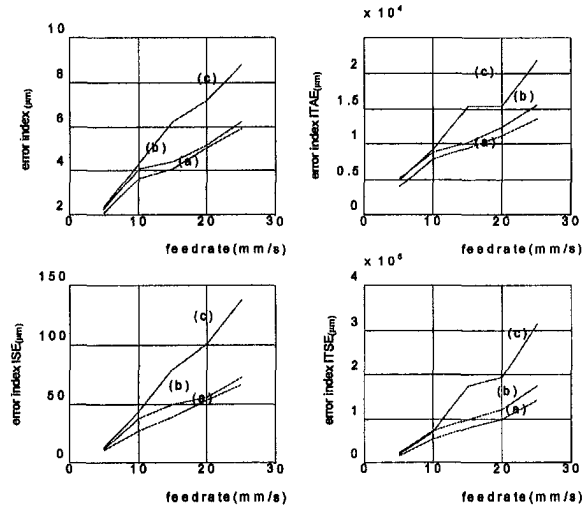

Fig. 17 The error index of three kinds of tool path obtained by CCPM tracking. Path was generated by (*a*) extended involute, (*b*) cubic spline fitting, (*c*) circular interpolation (Shpitalni et al., 1994).

3. Counter (16 bits up/down): IC model: HCTL-2016 (Operating frequency: 14 MHz)
4. Interface: 8255 board
5. D/A IO card (A626): D/A: 3 channels; output range: −10 V to +10 V; resolution: 12 bits
6. DC servomotors: Model: MT22G2-19; Volt Constant: 2 V/krpm; Max. Speed: 5000 rpm

The extended involute scroll contours generated by different tool-path generating method are executed at speeds of 5, 10, 15, 20, 25 mm/s. The experiment sampling time was 5 ms and each experimental duration was 5 seconds. A series of experiments was performed to track the three types of tool-paths with four different control schemes. Furthermore, the experiment results was quantified by the error indices of IAE, ITAE, ISE, ITSE.

4.2.1 CCPM Versus US, PPM, and CCS. CCPM prevailed over US, PPM and CCS in tracking all three types of tool-path, i.e., (*a*) generated by extended involute, (*b*) generated by cubic spline fitting, (*c*) generated by circular interpolation (Shpitalni et al., 1994). Figures 10–15 showed that CCPM left the smallest magnitude of contour error $|\epsilon_{max}|$ 16.4952, 17.2065, 19.8700 μm for feedrate 5 mm/s, 26.0390, 26.6673, 30.0190 μm for feedrate 10 mm/s, 26.7530, 31.7632, 33.3790 μm for feedrate 15 mm/s, 29.1780, 32.2742, 36.3840 μm for feedrate 20 mm/s, 31.8840, 33.2675, 42.1890 μm for feedrate 25 mm/s. Also, CCPM had the smallest error index of IAE, ITAE, ISE, ITSE as shown in Figs. 11, 13, and 15. Tables 1–3 compared the experimental results from US, CCS, PPM, CCPM for three kinds of tool-paths at feedrate 10 mm/s. The $|\epsilon_{max}|_{CCPM}/|\epsilon_{max}|_{US}$ ratio of three kinds of tool-paths are 0.52, 0.54, 0.58, the ratio of $|\epsilon_{max}|_{CCPM}/|\epsilon_{max}|_{CCS}$ ratio of three kinds of tool-paths are 0.9, 0.78, 0.89, the $|\epsilon_{max}|_{CCPM}/|\epsilon_{max}|_{PPM}$ ratio of three kinds of tool-paths are 0.92, 0.79, 0.89. Also, the error index ratio of CCPM/US, CCPM/CCS and CCPM/PPM vary from 0.3 ~ 0.92 as shown in Tables 2–4. The experimental results suggested that the CCPM performed best among US, CCS, PM, CCPM for tracking three kinds of tool-paths.

4.2.2 Extended Involute Versus Fitting and Interpolation as Tracked by CCPM. As shown in Figs. 16 and 17, tracking tool-path generated by extended involute with CCPM provided the smallest contour error $|\epsilon_{max}|$ for feedrate 5~25 mm/s. As shown in Tables 4 and 5, the contour error ratio of $|\epsilon_{max}|_{(a)}/|\epsilon_{max}|_{(b)}$ varies from 0.82~0.96, the error index of $IAE_{(a)}/IAE_{(b)}$ varies from 0.89~0.97, the error index of $ITAE_{(a)}/ITAE_{(b)}$ varies from 0.79~0.93, the error index of $ISE_{(a)}/ISE_{(b)}$ varies from 0.79~0.93, and the error index of $ITSE_{(a)}/ITSE_{(b)}$ varies from 0.73~0.82 for feedrate 5 mm/s~25 mm/s. Furthermore, the contour error ratio of $|\epsilon_{max}|_{(a)}/|\epsilon_{max}|_{(c)}$ varies from 0.76~0.87, the error index of $IAE_{(a)}/IAE_{(c)}$ varies from 0.66~0.89, the error index of $ITAE_{(a)}/ITAE_{(c)}$ varies from 0.61~0.87, the error index of $ISE_{(a)}/ISE_{(c)}$ varies from 0.48~0.87, and the error index of $ITSE_{(a)}/ITSE_{(c)}$ varies from 0.45~0.86 for feedrate 5 mm/s~25 mm/s. From above discussion, it is obvious that tracking tool-path generated by extended involute equation in terms of time with CCPM provided best precision.

It is interesting to find that better path generation brings more precision than better tracking methodology. As can be seen from Fig. 10 and Fig. 14, path generated by the proposed extended involute algorithm Eq. (2.14) enabled PPM and CCS to confine maximum contour error below 35 μm at all feedrates, while path generated by circular interpolation, even tracked by CCPM, issued bigger maximum contour errors especially at higher feedrates. This fact tells the importance of developing a better path generation algorithm to enhance the overall profile precision in CNC technology.

5 Conclusions

Curve fittings and interpolations are well established techniques for profile machining in CNC technology. The convenience of these mature industry standards is obtained at the cost of errors in profile/tool path generation. These errors were suppressed to the best possibility by different schemes of position control and contour control among which the cross-coupling system (CCS) has been proven very effective. The path precompensation (PPM) is an idea that executes a rate modification ahead of position control. More parts of the motion mechanism are included within the feedback loop. This feature makes PPM effective in dealing with curves with significant curvature. CCPM combines both advantages to form a new powerful tracking methodology which stands out especially at high feedrates.

However, CCPM requires a trajectory/tool path algorithm specifically derived from the exact mathematical curve equation. This is not always straightforward. This paper discussed the transform of a curve from parameter form to time base form. The extended involute scroll for industrial compressor is selected as the target profile. Specific profile (tool path) algorithm for extended involute scroll was proposed following the general approach of time base transformation. Comparisons with curve fittings and with the latest interpolation method were given and the precision of the proposed path algorithms was

Table 5 The experimental comparison of different tool-path tracked by CCPM

Feedrate (mm/s)	$\lvert\epsilon_{max}\rvert_{(a)}/\lvert\epsilon_{max}\rvert_{(c)}$	$IAE_{(a)}/IAE_{(c)}$	$ITAE_{(a)}/ITAE_{(c)}$	$ISE_{(a)}/ISE_{(c)}$	$ITSE_{(a)}/ITSE_{(c)}$
5	0.83	0.89	0.81	0.87	0.86
10	0.87	0.84	0.87	0.62	0.76
15	0.8	0.66	0.61	0.49	0.45
20	0.8	0.70	0.73	0.53	0.50
25	0.76	0.67	0.62	0.48	0.45

confirmed. The proposed algorithm was also implemented and tracked by CCPM in experiments. The results showed that the proposed algorithm tracked by CCPM performed best among known methodologies.

Since most curves can be represented in parametric form, the approach shown in this paper open the possibility of quasi-generalization of the path algorithm establishment for CCPM. Thus makes the CCPM a widely applicable precision tracking methodology.

Acknowledgments

The authors thank the National Science Council of the Republic of China for the support of this research under Grant No. NSC-86-2212-E-009-031.

References

Chin, J.-H., and Tsai, H.-C., 1993, "A Path Algorithm for Robotics Machining," *Robotics & Computer-Integrated Manufacturing,* Vol. 10, pp. 185–198.

Chin, J.-H., and Lin, T.-C., 1997, "Cross-coupled Precompensation Method for the Contouring Accuracy of CNC Machine Tools," *Int. J. Machine Tools and Manufacture,* Vol. 37, No. 7, pp. 947–967.

Chin, J.-H., and Liu, Y.-R., 1997, "Cross-Coupled Precompensation Method for Tracking High Order Curves," Report from Cutting Lab., Institute of Mechanical Engineering, National Chiao Tung Univ., Taiwan, ROC.

Chin, J.-H., and Lin, S.-T., 1997, "The Path Precompensation Method for Flexible Arm Robot," *Robotics and Computer Integrated Manufacturing,* Vol. 13.

Chin, J.-H., and Tsai, H.-C., 1997, "Path Precompensation Algorithm for Robotic Machining of Spatial Curves and Surfaces," *Proceeding of the IASTED Int. Conference on Applied Modelling and Simulation,* July 27–Aug. 1, Banff, Canada, pp. 272–275.

Chou, J. J., and Yang, D. C. H., 1992, "Command Generation for Five-Axis CNC Machining," ASME *Journal of Engineering for Industry,* Vol. 114, pp. 15–21.

Chung, J. H., and Liu, C. H., 1991, "Cross-Coupled Adaptive Feedrate Control for Multiaxis Machine Tools," ASME JOURNAL OF DYNAMIC SYSTEMS, MEASUREMENT, AND CONTROL, Vol. 113, pp. 451–457.

Chung, J. H., and Liu, C. H., 1992, "A Model-Reference Adaptive Control Strategy for Improving Contour Accuracy of Multi-axis Machine Tools," *IEEE Transaction of Industry Application,* Vol. 28, pp. 221–227.

Feng, L., Koren, Y., and Borenstein, J., 1993, "Cross-Coupling Motion Controller for Mobile Robots," *IEEE Control Systems,* pp. 35–43.

Huan, J., 1982, "Bahnregelung zur Bahnerzeugung an numerisch gesteuerten Werkzeugmaschinen," Dissertation, University of Stuttgart.

Huang, S. J. and Chen, C. C., 1995, "Application of Self-tuning Feed-Forward and Cross-Coupling Control in a Retrofitted Milling Machine," *Int. J. Machine Tools Manufacture,* Vol. 35(4), pp. 577–591.

Isermann, R., 1987, *Digitale Regelsysteme,* Band I, Springer-Verlag Berlin Heidelberg.

Ishii, N., Yamamura, M., Muramatsu, S., Yamamoto, S., and Manabu, S., 1990, "Mechanical Efficiency of a Variable Speed Scroll Compressor," *Proceedings of the International Compressor Engineering Conference at Purdue,* pp. 192–199.

Koren, Y., 1979, "Design of Computer Control for Manufacturing Systems," ASME *Journal of Engineering for Industry,* Vol. 101.

Koren, Y., 1980, "Cross-Coupled Biaxial Computer Control for Manufacturing," ASME JOURNAL OF DYNAMIC SYSTEMS, MEASUREMENT, AND CONTROL, Vol. 102(4), pp. 265–272.

Koren, Y., and Lo, C. C., 1991, "Variable-Gain Cross-Coupling Controller for Contouring," *Annals of the CIRP,* Vol. 40(1), pp. 371–374.

Kulkarni, P. K., and Srinivasan, K., 1989, "Optimal Contouring Control of Multi-Axial Feed Drive Servomechanisms," ASME *Journal of Engineering for Industry,* Vol. 111, pp. 140–148.

Kulkarni, P. K. and Srinivasan, K., 1990, "Cross-Coupled Control of Biaxial Feed Drive Servomechanisms," ASME JOURNAL OF DYNAMIC SYSTEMS, MEASUREMENT, AND CONTROL, Vol. 112(2), pp. 225–232.

Lin, R. S., and Koren, Y., 1996, "Efficient Tool-Path Planning for Machining Free-Form Surfaces," ASME *Journal of Engineering for Industry,* Vol. 118, pp. 20–28.

Masory, O. and Koren, Y., 1982, "Reference-Word Circular Interpolators for CNC Systems," ASME *Journal of Engineering for Industry,* Vol. 104, pp. 400–405.

Nakamura, S., 1993, *Applied Numerical Methods in C,* Englewood Cliffs, N.J., Prentice Hall.

Sarachik, P. and Ragazzini, J. R., 1957, "A Two Dimensional Feedback Control System," *Trans. AIEE,* Vol. 76, pp. 55–61.

Shieh, Y. S., Lee, A. C., and Chen, C. S., 1996, "Cross-Coupled Biaxial Step Control for CNC EDM," *Int. J. Machine Tools and Manufacture,* pp. 1–21.

Shpitalni, M., Koren, Y., and Lo, C. C., 1994, "Realtime Curve Interpolators," *Computer-Aided Design,* Vol. 26(11), pp. 832–838.

Tomizuka, M., Anwar, G., and Tung, E. D, 1993, "Low Velocity Friction Compensation and Feedforward Solution Based on Repetitive Control," ASME JOURNAL OF DYNAMIC SYSTEMS, MEASUREMENT, AND CONTROL, Vol. 115, pp. 279–284.

Tseng, C. H. and Lia, C. F., 1994, "Optimum Design of the Extended, Involute Scroll Curve," Report from Optimum Lab., Institute of Mechanical Engineering, National Chiao Tung Univ., Taiwan, ROC.

Tseng, C. H. and Shih, Y. P., 1995, "Optimum Design of the Extended Involute Scroll Seal," Report from Optimum Lab, Institute of Mechanical Engineering, National Chiao-Tung Univ., Taiwan, ROC.

Yang, L-F, and Chang, W-H, 1996, "Synchronization of Twin-Gyro Precession Under Cross-Coupled Adaptive Feedforward control," *Journal of Guidance, Control, and Dynamics,* Vol. 19(3), pp. 534–539.